Energetic Influence of Motor Power in Drive Systems with Space-Vector Static Converters and Induction Motors

Mihăiță Lincă, Constantin Vlad Suru and Alexandru Bogdan Lupu
University of Craiova/Electrical Engineering Faculty, Craiova, Romania, mlinca@em.ucv.ro

Abstract **–The static converters are a vital component of modern drive systems, which in turn are indispensable in industrial equipment designed for small or large complexity, because the achievement of finished goods implies the adjustable mechanical energy available at the output of the system. The aim of this paper is the energetic analysis of two drive systems with the same static converter feeding two different motors which had been performed on an experimental stand for different static operating points. It was considered feeding the both asynchronous motors from the static converter using the space vector modulation command strategy while the mechanical load was assured by a special braking machine and by a DC motor, respectively. It had been taken into consideration feeding the both motors at the same frequencies and with the same RMS voltages. The frequencies considered for the energetic analysis are 20Hz, 30Hz, 40Hz and 50Hz, the mechanical load being adjusted from no load operation up to the nominal value. The power grid energetic parameters were recorded using a Fluke 41b harmonic analyzer, while the current and voltage waveforms at the motor input, were recorded using a Metrix Ox704 digital oscilloscope and later used in Matlab to calculate the AC electric powers.**

Keywords: *electric drive, static converter, induction motor, quality indicators, PWM modulation.*

I. INTRODUCTION

Starting from the square-wave modulation the space vector modulation appeared and improved to minimize copper losses, torque ripple, etc. Space vector modulation techniques used today to control the modern static converters as part of high–power machine drives, strongly depend on switching frequency of the power semiconductors.

The electric drive is an essential component of technical equipments for industrial activities of high or low complexity, because machining towards the final product requires the mechanical energy available from the drive system.

This paper is dedicated to the study of the influence of the motor power to the overall drive system energetic performances.

Though, in the first section, a brief description of the theoretical definitions is given regarding the inverter adopted modulation strategy and the power quality indicators which were used in this study. In the next section, the experimental setup and protocol was described, followed by the experimental results, given in the last section.

II. THEORETICAL ASPECTS

A. Space Vector Modulation

The space vector modulation working principle is based on the idea that for a system to provide sinusoidal output voltages, the associated voltage space vector must rotate continuously. If the sinusoidal voltage frequency and amplitude are constant, the locus of peak vector is a circle.

Because the operation of the inverter permits only eight possible configurations, due to the "on" and "off" function of semiconductor devices, the voltage vector can only have eight distinct positions, 6 non-zero ($\underline{u}_1$, $\underline{u}_2$, $\underline{u}_3$, $\underline{u}_4$, $\underline{u}_5$, $\underline{u}_6$) which correspond to vertexes of a regular hexagon and the other two ($\underline{u}_7$, $\underline{u}_8$) are null and corresponding to the center of the hexagon- [4], [8].

B. Power quality indicators

Because the quality indicators that were used required the active power absorbed by the motor in each static operating point, for computing the active power the complex apparent power theory [1] (p-q theory) had been used.

According to the p-q theory, the instantaneous complex apparent power is defined as the product of the voltage phasor (u) and the complex conjugate of the current phasor (i*) [2]:

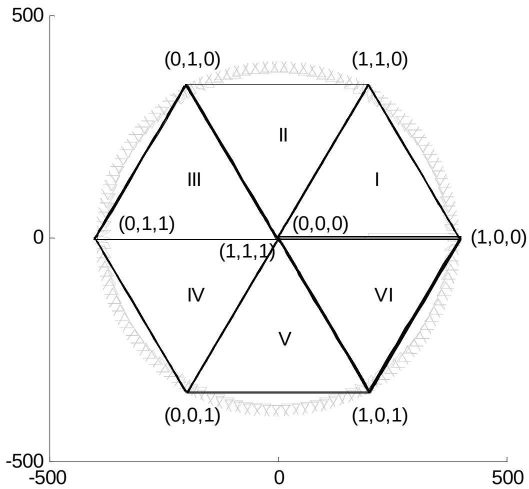

Fig. 1. The associated voltage space vector of the inverter output.

$$\underline{s} = p + jq = \frac{3}{2}\underline{u}\cdot\underline{i}^* = \\ = \frac{3}{2}\left[u_d i_d + u_q i_q + j\left(-u_d i_q + u_q i_d\right)\right] \quad (1)$$

where the real power is:

$$p = \frac{3}{2}\left(u_d i_d + u_q i_q\right) \quad (2)$$

Is widely accepted that the average value of the real power, p, over one period (T) gives the active power P:

$$P = \frac{1}{T}\int_{t-T}^{t} p dt \quad (3)$$

It's also widely accepted that that the average value of the imaginary part q, over one period of the voltages and currents (T) gives the reactive power Q:

$$Q = \frac{1}{T}\int_{t-T}^{t} q dt \quad (4)$$

Starting from the instantaneous complex aparent power, the aparent power can be defined [5], [7], keeping true Bucholtz's formula [3]. Thus:

$$S_f = \sqrt{\frac{1}{T}\int_{t-T}^{t} \frac{U^2}{|\underline{u}|^2}|\underline{s}|^2 dt} \quad (5)$$

where $\underline{\boldsymbol{U}}^2$ is the square RMS value of the voltage phasor modulus,

$$U^2 = \frac{1}{T}\int_{t-T}^{t} |\underline{u}|^2 dt \quad (6)$$

So, the aparent power is given by:

$$S_f = \sqrt{\frac{1}{T}\int_{t-T}^{t} \frac{U^2}{|\underline{u}|^2}\frac{9}{4}|\underline{u}|^2|\underline{i}|^2 dt} = \frac{3}{2}UI \quad (7)$$

Considering the quadrature relationship between powers, the distorsion power is defined as [6]:

$$D_f^2 = S_f^2 - P^2 - Q^2 \quad (8)$$

Knowing the active power absorbed by the motor, the efficiency can be obtained, after the computation of the mechanical power:

$$\eta = \frac{P_m}{P} \quad (9)$$

$$P_m = T \cdot \Omega \quad (10)$$

where: T is the torque and Ω is the angular velocity, measured at the motor shaft. Because the experimental equipment allowed only the measurement of the motor RPM, n, the angular velocity was calculated with:

$$\Omega = \frac{\pi \cdot n}{30} \quad (11)$$

III. Experimental Setup And Protocol

A. *The experimental setup*

To obtain the experimental data required to determine the energetic performances of each drive system, a Leybold type experimental stand was used [9]. It contains (Fig. 2, Fig. 3):

- single phase full wave bridge rectifier;
- DC link;
- three phase voltage inverter with IGBTs and its control module;
- squirrel cage asynchronous motor;
- mechanical load (asynchronous motor of special construction and its torque control module used with the first, lower power motor, and a DC motor for the second, higher power motor);
- digital analysis equipment (Fluke 41b analyzer, Metrix OX 7042 – M digital oscilloscope, etc).

The power system components have the nominal operated data indicated below:

- Motor1: P_N=370W; U_N = 230V; I_N = 2.1A; cosφ = 0.76; n_N = 1380 rot/min.
- Motor2: P_N=2.2kW; U_N = 230V; I_N = 10A; cosφ = 0.92; n_N = 1500 rot/min.
- Inverter: U_N = 230V; I_N = 10A.
- Load1: P_N=250W; U_N =230V; T_N=2Nm.
- Load2: P_N=2.7kW; U_N =230V; T_N=18Nm.

To obtain the experimental data required to determine the energetic performances of induction motors powered by space vector modulation voltage inverters the measurement of the DC-Link voltage and current was required to obtain the intermediary DC power.

The power grid energetic indicators were computed by the Fluke 41b analyzer and the energetic parameters on the motor side were computed based on the voltage and current waveforms using a Matlab/Simulink model.

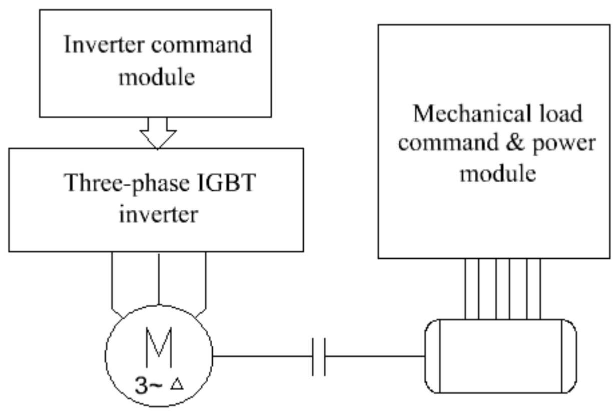

Fig. 2. The drive system block diagram.

B. *The experimental protocol*

For the experimental protocol, two cases had been taken into consideration [11]:

- Feeding the motors with the same RMS voltages;
- Feeding the motors in order to achieve the same static torque.

The frequencies considered for the energetic analysis are 20Hz, 30Hz, 40Hz and 50Hz, for which the load was adjusted up to the nominal value.

For the lower power motor (P_N=370W) the mechanical load was a asynchronous motor of special construction and its torque control module. The mechanical load of the higher power motor (P_N=2.2kW) was a DC motor (P_N=2.7kW) used as generator feeding a high power variable resistor.

Through the experimental protocol, in order to compute the energetic performances of the two motors the line voltage and current waveforms were digitally recorded using a digital oscilloscope.

Further, in Matlab / Simulink, the waveform of voltages and currents were reconstructed based on the sampled stored by the digital oscilloscope and the following quantities were computed: the active power, at the power grid side and on the motor side, the mechanical power at the motor shaft and the efficiency of the drive system for feeding the motor at constant frequency (20, 30,40 and 50 Hz) and different values of the load torque (0; 0.1 ;0.2; 0.3; 0.4;0.5;0.6;0.7;0.8;0.9; 1;1.1) T_N.

Taking into account the experimental protocol and starting from measured data for each static operating point, the other quantities needed to determine the energetic performances were calculated and the comparative analysis could be achieved.

For each operating point besides the waveforms of voltage and current some quantities had been measured using classical equipment: the RMS values of voltage and current, active power, rotor revolution count (RPM), and torque, respectively.

Fig. 3. The experimental workbench.

IV. Experimental Setup

The energetic performances were analyzed based on the measured quantities and on the quantities computed in Simulink from the motor side waveforms, at the same frequency (20, 30, 40 and 50 Hz) and for the same RMS voltage values. The graphical variation for the most significant energetic quality indicators was illustrated using Matlab.

Therefore, the dependence of efficiency by the mechanical power is illustrated in Fig. 4 for the lower power motor, and in Fig. 5, for the higher power motor. It can be seen that the second motor gives a better efficiency, because of its higher nominal power, at all the working frequencies, excepting for 30 Hz, where the first, lower power motor gives the best efficiency. Also, the bigger motor gives a flatter efficiency over the mechanical power variation while the smaller motor gives a curved, pointed dependence (the maximum efficiency is reached at about 280W, which is 75% of the nominal power, and drops steeply).

The torques, generated by the motors of the two studied drive systems, are illustrated in Fig. 6 and Fig. 7. It can be seen that de torque dependence of the mechanical power at the motor shaft is almost linear for all frequencies.

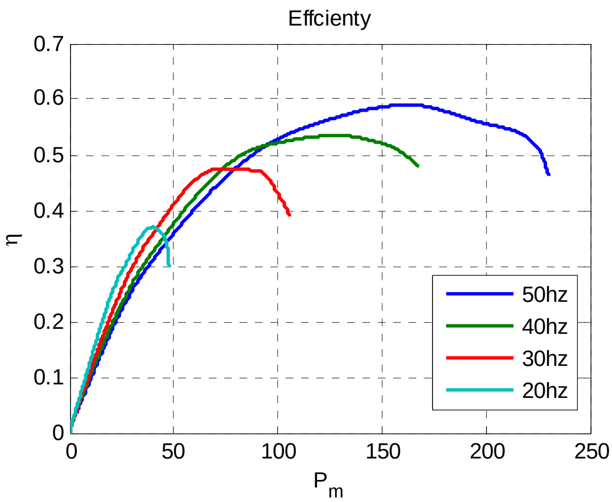

Fig. 4. Efficiency of the motor 1 as a function of mechanical power.

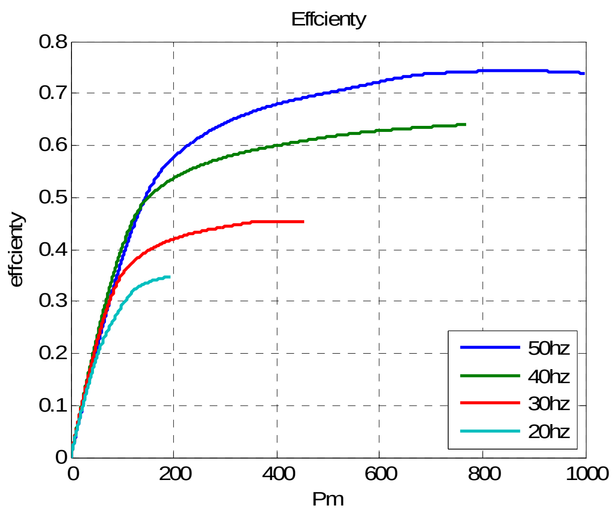

Fig. 5. Efficiency of the motor 2 as a function of mechanical power.

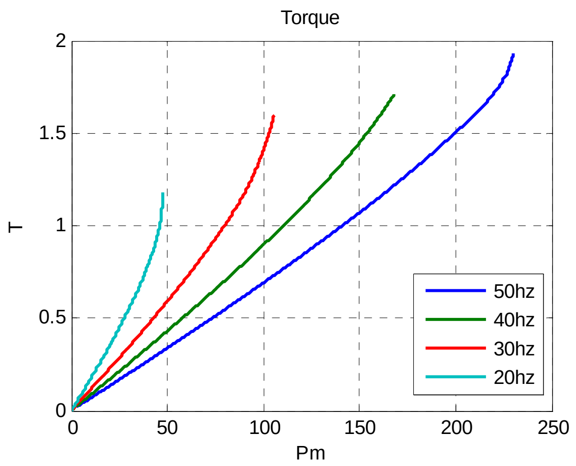

Fig. 6. Torque of the motor 1.

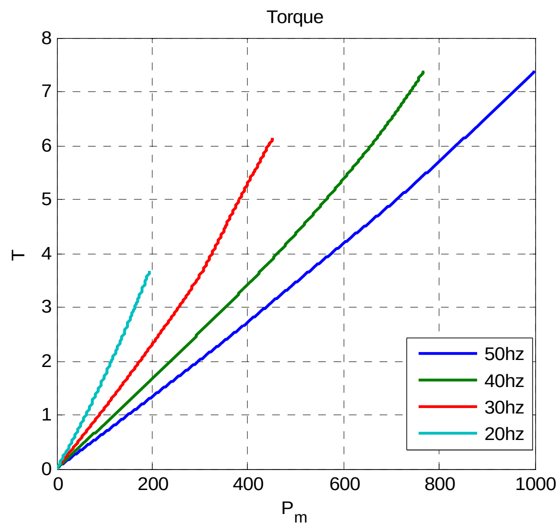

Fig. 7. Torque of the motor 2.

It can be seen, although, that when the motor load is increased up to the maximum value the generated torque dependence is becoming nonlinear, the torque being relatively higher than for lower output power. This nonlinearity is more emphasized for the higher power motor and is reflected in the dependence of the rotor speed as a function of mechanical power.

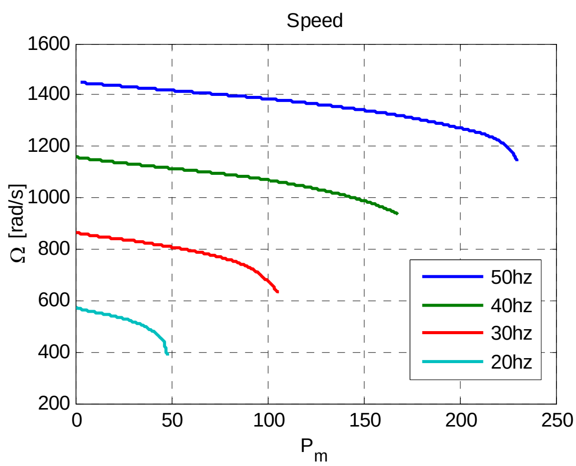

Fig. 8. Speed of the motor 1.

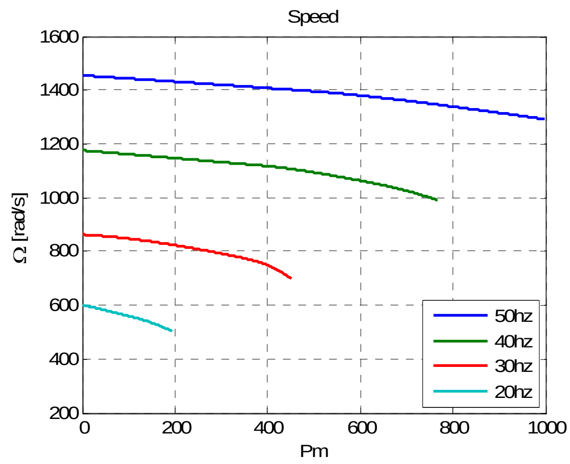

Fig. 9. Speed of the motor 2.

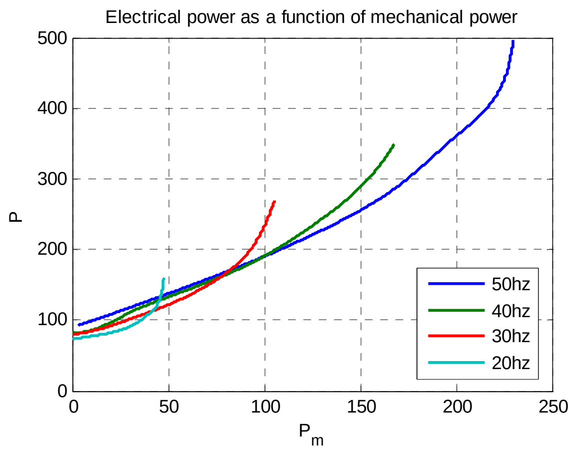

Fig. 10. Electrical power of the motor 1 as a function of mechanical power.

It appears that the graphical dependence of torque and rotor speed of the low power motor by the mechanical power is as to be expected, in the case of the high power motor the results are not as expected.

It can be observed that the torque is increasing rapidly at high mechanical power while the rotor speed is decreasing rapidly.

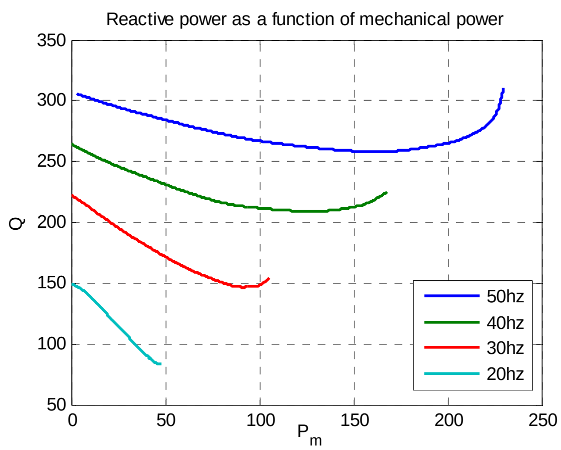

Fig. 11. Reactive power of the motor 1 as a function of mechanical power.

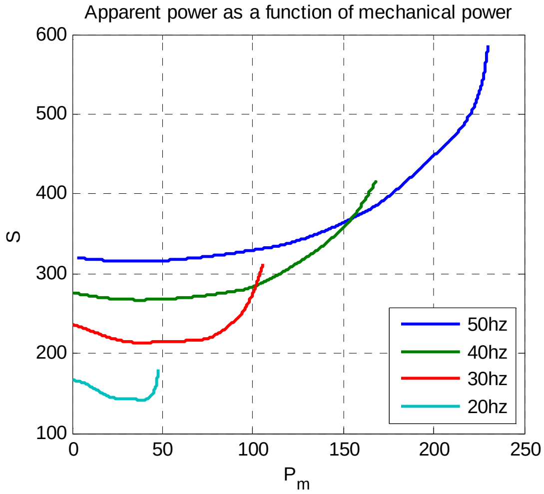

Fig. 12. Apparent power of the motor 1 as a function of mechanical power.

The dependence of the angular velocity of the motor on the mechanical power is illustrated in Fig. 8 for the low power motor and in Fig. 9 for the high power motor. It results for the latter, that the rotor speed dependence of this motor is flatter and less dropping than for the low power motor.

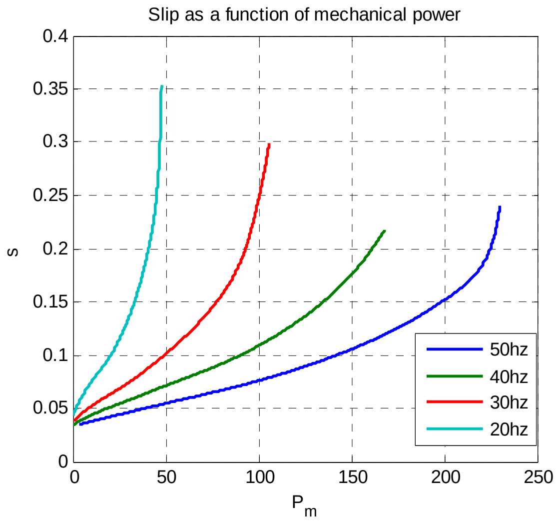

Fig. 13. Slip of the motor 1 as a function of mechanical power.

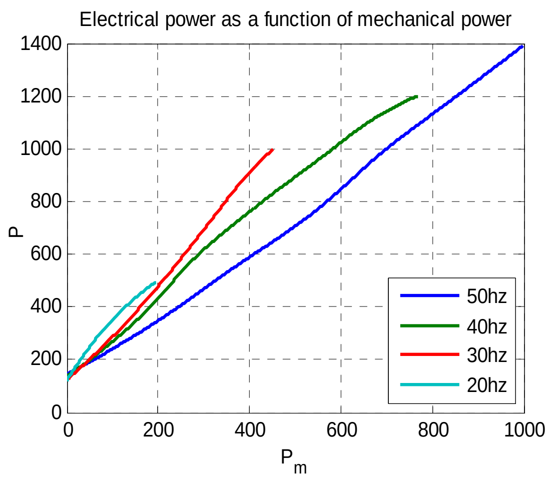

Fig. 14. Electrical power of the motor 2 as a function of mechanical power.

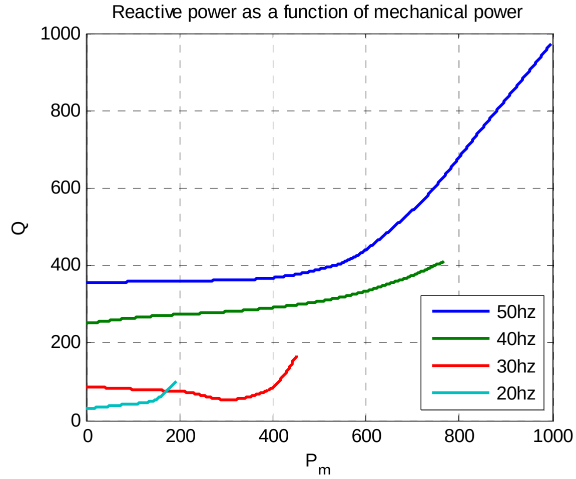

Fig. 15. Reactive power of the motor 2 as a function of mechanical power.

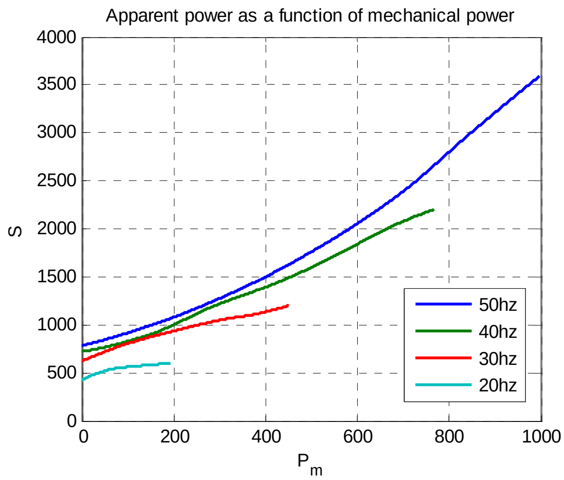

Fig. 16. Apparent power of the motor 2 as a function of mechanical power.

At the same mechanical power, for high frequencies, the first motor reactive power is lower than the second motor (Fig. 11,Fig. 15).

For the same frequency and mechanical power, the apparent power, at the first motor, is higher than the one at the second motor (Fig. 12,Fig. 16). This is because, the last motor has a higher rated electric power.

For the same mechanical power, the first motor electric power is lower than the second motor corresponding power (Fig. 10, Fig. 14). It can be noticed that the electric power is higher at lower frequencies. The slip of the motor increases with the frequency decreasing (Fig. 13).

V. Conclusions

It results that the drive system performances are dependent on the used induction motor, besides the obvious maximum mechanical power, but also regarding the shape of the dependences of efficiency, torque and rotor speed, by the shaft mechanical power.

The determinations were conducted for the same static converter, with the same inverter modulation strategy, and for a generic mechanical load, giving a prescribed reverse torque, for a typical or generic variation.

It seems that when using a lower power motor the efficiency not only is lower, as expected, but also much curved, pointed dependence on the shaft mechanical power.

Also, the rotor speed variation is much biased for the low power motor, while the high power one is flatter, less biased, by with a steep drop a the upper limit of the rotor mechanical power.

ACKNOWLEDGMENT

This work was performed through the program Partnerships in priority areas — PN II, conducted with the financial support of MEN – UEFISCDI, project no. PN-II-PT-PCCA-2013-4-0564 (42/01.07.2014).

The authors gratefully acknowledge the contributions of Prof. Alexandru Bitoleanu for his work on the original version of this document.

Received on July 20, 2015

Editorial Approval on November 28, 2015

REFERENCES

[1] V.N. Nedelcu, *Electromechanical conversion theory,* Technical Ed., Bucharest, 1978. (In Romanian)

[2] H. Akagi and A. Nabae, *The p-q theory in three-phase systems under non-sinusoidal conditions,* European Trans. on Electrical Power, 3 (1993), No.1, 27-31.

[3] F. Buchholz, *Die Drehstrom-Scheinleidtung bei ungleichmä√iger Belastung der drei Zweige. Licht u. Kraft*, Org. Elektrotech. Ver München, No.2, 1922.

[4] A. Bitoleanu, Mihaela Popescu, D. Mihai, C. Constantinescu, *Static converters and high performance control structures,*(in Romanian) Ed. SITECH, Craiova 2000, pp.48 – 70.

[5] A. Bitoleanu, Mihaela Popescu and V. Suru: *P-Q Power Theory: Some Theoretical and Practical Aspects,* Proceedings of 10th International School on Nonsinusoidal Currents and Compensation 2010 (ISNCC 2010), pp. 10-15, June 15-18, Lagow, Poland, ISBN 978-1-4244-7894-1.

[6] Mihaela Popescu, A. Bitoleanu, M. Dobriceanu, M. Linca, *Energy-efficient inverter-fed induction motor driving system,* Proceedings of IEEE International Electric Machines and Drives Conference, IEMDC 2007, v 2, 2007, p 1685-1688. (INSPEC).

[7] M. Lincă, Vlad Suru, *Power quality in drive systems based on space-vector controled static converters and induction motors,* Annals of the University of Craiova, Serie Electrical engineering, No.34, Vol.II, 2010, ISSN-1842-4805, pp.200-205 .

[8] M. Lincă, *Research on drive systems with asynchronous motor and voltage and frequency PWM static converters,* PhD Thesis, University of Craiova, 2010.

[9] G. F. v Schlotheim, *Frequency Converter Technology,* Drives, Leybold Didactic GmbH.

[10] Wen-Chang Tsai, *Estimation of Core Losses in an Induction Motor under PWM Voltage Excitations Using Core Loss Curves Tested by Epstein Specimens,* International Forum on Systems and Mechatronics, 20.

[11] Mihaita Linca, Alexandru Bitoleanu, Lupu Alexandru-Bogdan *Experimental energetic analysis of electrical drive system with induction motor and space vector modulation* SIELMEN 2013.